SCA2003-14: RESIDUAL GAS SATURATION OF SAMPLE ORIGINALLY AT RESIDUAL WATER SATURATION IN HETEROGENEOUS SANDSTONE RESERVOIRS

SUZANNE Karine (Ecole des Mines de Paris), HAMON Gérald (Total),
BILLIOTTE Joël (Ecole des Mines de Paris), TROCME Vincent (GazdeFrance)

ABSTRACT

Residual gas saturation is known to be a key factor in evaluating gas recovery from a lean gas reservoir invaded by water. The large scatter in maximum trapped gas saturation (SgrM), the existence of two opposite SgrM/porosity trends and the key controls of the variability of SgrM were illustrated by two recent studies (Suzanne et al., 2001; Hamon et al., 2001). This paper tackles the influence of irreducible water saturation on the variability of trapped gas saturation.

Sgr measurements were performed by controlled evaporation and capillary imbibition or by capillary drainage/imbibition. Sixty samples were selected from sandstone formations to account for the largest scatter in SgrM observed in our previous study and cover a very large range in porosity and permeability. The main results of this study are:

- The fluid distribution after controlled evaporation was checked with NMR and X-ray scanner measurements and was found homogeneous.

- The Sgr values obtained by evaporation-imbibition were found in very close agreement with those achieved by capillary drainage - imbibition on eight reservoir samples

- The presence of irreducible water prior to the imbibition does not change the existence of two opposite Sgr trends as a function of porosity (or permeability).

- Sgr at irreducible water saturation, Sgr@Swir, may decrease as porosity decreases. This relationship is shown to be related to increasing clay content, decreasing pore size or increasing amount of microporosity as SgrM values.

- Maximum trapped gas saturation and Sgr at irreducible water saturation were found equal. So, Sgr may either increase or decrease as a function of irreducible water saturation, showing that Sgr is not controlled only by initial water saturation. And, the frequent extrapolation of Land's empirical relationship to the interval [SgrM, Sgr@Swir] is not correct.

INTRODUCTION

During depletion of gas fields, the aquifer often encroaches into the reservoir, and residual gas saturation (Sgr) is used to estimate microscopic recovery. The authors have shown in previous papers [1; 2] that SgrM values vary between 0.05 and 0.95. Yet, the economic impact of Sgr on gas reservoir can be extremely high.

Many studies have attempted to understand gas-trapping mechanisms. First, Geffen et al.[3] established that residual gas saturation measured in the laboratory on core samples is the same as in a gas reservoir. Later results [4 to 8] proved that simple experimental conditions may be representative of gas trapping in reservoirs. As the objectives of this study are to gather a substantial number of experimental results over a large range of rock characteristics, simple experimental conditions are advisable. In this work, trapped gas saturations are obtained by spontaneous imbibition at ambient conditions on samples.

Many studies have tried to correlate trapped gas saturation to reservoir characteristics [3 to 10]. Katz et al. [6] have underscored a relationship between SgrM and porosity: as porosity increases, SgrM decreases. Following authors have confirmed this single but scattered trend [5 to 10]. In the previous papers [1; 2], we have presented a new trend SgrM-porosity; and we have shown the influence of microporosity and pore size on SgrM values. To complete this study and achieve more representative results, we have focused this work on the influence of maximum initial gas saturation on residual gas saturation.

Crowell et al. [4] illustrated the effect of initial gas saturation (Sgi) on trapped gas saturation (Sgr). Land [11] proposed the well known relationship:

$$\frac{1}{S_{gr}^*} - \frac{1}{S_{gi}^*} = C = \frac{1}{Sgr@Swir} - \frac{1}{1-Swir} \tag{1}$$

S_{gi}^* and S_{gr}^* are effective gas saturations expressed as a fraction of pore volume excluding the pore volume occupied by the irreducible wetting phase, Swir:

$$S_{gi}^* = \frac{S_{gi}}{1-Swir} \text{ and } S_{gr}^* = \frac{S_{gr}}{1-Swir} \tag{2}$$

C parameter is Land's coefficient which is assumed to be only rock dependent. Its value is defined by the end point of the Sgi -Sgr curve.

A simplified form of Land's law, based on real gas saturation, is commonly used:

$$\frac{1}{S_{gr}} - \frac{1}{S_{gi}} = C = \frac{1}{SgrM} - 1. \tag{3}$$

Combination of equations (1) and (3) leads to a relationship that links SgrM, Swir and Sgr@Swir:

$$\frac{1}{Sgr@Swir} - \frac{1}{1-Swir} = C = \frac{1}{SgrM} - 1 \tag{4}$$

Very often, Sgr@Swir is estimated by using equation (4). This implies the two values (SgrM and Sgr@Swir) are different and Sgr@Swir is a function of Swir.

Some authors [12; 13] underscored a relationship between Sgr@Swir and Swir (Figure 1A) unlike Chierici et al. [8] Few authors [3; 7; 14] have concluded that Sgr@Swir is close to SgrM based on few experimental data (Figure 1B) unlike the idea of most of the authors as Crowell et al.[4]

Sgr-Sgi relationships are determined by carrying out a set of drainage-imbibition sequences. The drainage allows to get the value of Sgi and the end point of the following imbibition defines the corresponding value of Sgr. Two methods were used for getting Sgi: capillary desorption and controlled evaporation. The present work studies the effect of the methods used to get to Sgi on Sgr values (drainage-imbibition or evaporation-imbibition), and, then the Sgr@Swir values as a function of some petrophysical parameters.

EXPERIMENTS

Core Samples

Sixty samples were selected from two gas reservoirs of the Far East (M1 and M3) and from Fontainebleau Sandstone outcrops (FTB). Cylindrical samples of different lengths, and 23 mm or 40 mm in diameter, were cut from whole core samples. Their porosity and permeability range respectively from 0.06 to 0.25 and from 0.1 to 3 000 mD. Figure 2 illustrates permeability versus porosity and SgrM versus porosity samples position. It is important to note that this sampling covers a large range of combinations between pore network characteristics and maximum trapped gas saturation as illustrated by our previous work [1, 2].

Measurements

The following sequence was performed. 1- Samples were cleaned with chloroform by soxhlet extraction and dried at 80°C. 2- Matrix volume was measured either using a helium picnometer, or by hydrostatic weighing operation on chloroform-saturated samples 3- Bulk volume was measured by mercury hydrostatic weighing operation. 4- Gas permeability measurements. 5- Formation factor was measured on brine-saturated samples. 6- SgrM was measured as described in the next paragraph. 7- After Isopar L® saturation of samples, they are drained by controlled evaporation and Sgr is measured for each Sgi value as described below. 8- SgrM values are again measured for checking.

Residual Gas Saturation (Sgr) Measurement

Spontaneous imbibition was used for both Sgr and SgrM measurements. This technique was described and validated in previous papers [2, 3, 5]. Refined oil, Isopar L®, is used as wetting phase rather brines to avoid clay disturbance within the porous space. Isopar L® is a strongly wetting liquid for both outcrop and reservoir samples that were cleaned with chloroform before carrying out experiments. Because of the strong wettability of Isopar L® and its low viscosity (1.3 mPa.s), measured saturations may be assumed to be equivalent to those obtained by using gas-water couple [3 to 5, 15].

Spontaneous imbibition was performed by immersing the lowermost tip of the sample into wetting fluid and by measuring the change of weight versus time (Figure 3A). As samples are put in a closed chamber, Isopar L® evaporation influence is minimized. Change in gas saturation during imbibition is plotted against the square root of time. The intersection of capillary-dominated period and diffusion-dominated period lines was selected as the trapped gas saturation. Throughout all experiments, these two regimes always were clearly

observed regardless of the sample permeability or initial gas saturation. The influence of diffusion is very low as the ratio between slopes of the two lines is typically equal to 1/20.

Getting to Initial Gas Saturation (Sgi)

Two methods are used to get to Sgi: controlled evaporation and capillary desorption. Fluids are air and Isopar L$^®$ for both methods.

The capillary desorption is a steady state drainage by capillary pressure. This drainage method is time-consuming, and allows to study few samples. The controlled evaporation consists of two stages (Figure 3B). The sample is placed into an opened desiccator with Isopar L$^®$ which evaporates easily. When the target weight is reached, the sample is put into a closed desiccator with Isopar L$^®$ during 12 hours. As air around the sample is saturated by Isopar L$^®$ vapour, evaporation is blocked. The aim of this second phase is to get a homogeneous distribution of fluids within the sample by relaxing capillary pressure gradients.

For both methods of drainage, Sgi values are measured by weighing operations just before the capillary imbibition. To begin a set of Sgi-Sgr measurements, the sample is initially saturated under pressure with Isopar L$^®$. Sgr is only measured if the new initial gas saturation is higher than the previous one. In this way, imbibition experiments are done at ever increasing gas saturations (S_{gi}) to avoid capillary hysteresis effects.

Evaluation of Swir

As Sgr, values of irreducible wetting saturation are assumed to be those of irreducible water saturation (Swir). The controlled evaporation does not allow to determine Swir during drainage as residual wetting saturation must be nil if evaporation is complete. So for all samples, Swir values have been estimated by using a relationship between Swir and permeability [16]. Saturation values which are obtained with Purcell curves at various pressures, are presented as a function of Kg (Figure 4). Swir values that were measured by capillary desorption on seven samples of M1 reservoir, are close to values that are estimated by using Purcell curves with an equivalent capillary pressure of 2 bars (Figure 4). Then Swir values which are presented in following plots are estimated by using this experimental relationship. The two others relationships will be used for defining an uncertainty interval [Swir_min, Swir_max] associated to estimated Swir values.

RESULTS

The results consist of two major parts. First, the validation of the used procedure based on fluids distribution verification and Sgr values comparison according to the different methods to get to Sgi. Second, Sgr@Swir values are presented as a function of various parameters.

Fluid Distributions after Controlled Evaporation

Theoretically, after capillary drainage, fluids are distributed homogeneously within the sample without edge influence; and large pores are preferentially drained in the porous

media. To verify this, the fluids distribution has been observed with tomography and NMR acquisitions at various Sgi values on different samples. Used fluids are Isopar L® and air as well as other Sgr-Sgi measurements.

To get successive CT-scans during Sgr-Sgi measurements, a Fontainebleau Sandstone sample was used (Table 1). We have obtained scanning images at four different saturation states: dry sample (Sgi = 1), saturated sample (Sgi = 0) and at two intermediate Sgi values (Sgi = 0.85 and Sgi = 0.35). The images do not exhibit local saturation variations or saturation gradients due to sample edges influence (Table 2). To get NMR measurements at various Sgi values, two samples have been selected from M1 reservoir sandstone. T2 distribution plots (Figure 5) confirm that controlled evaporations firstly drain big pores as capillary drainages do.

These results do not underline any influence of controlled evaporation on the fluids distribution within the sample.

Sgr-Sgi Curves Comparison

The conventionally method to drain is the steady-state capillary desorption. Eight saturated samples are drained in individual cells under controlled capillary pressure. They come from M1 and M3 reservoir sandstones with a large range of permeability, porosity and SgrM. Four examples of Sgi-Sgr relationships are presented to compare the values obtained after controlled evaporation and after capillary desorption on the same sample (Figure 7). For each sample, both Sgi-Sgr curves superimpose.

This validates the controlled evaporation associated to a simple spontaneous imbibition to measure Sgr-Sgi relationships. Now, results obtained using this procedure are presented.

Sgr@Swir Values as a Function of Porosity and SgrM

Sgr@Swir values have been determined by reading the Sgr value corresponding to that of Swir. Although estimated Swir values had large uncertainty intervals (Figure 6B), the uncertainty of Sgr@Swir values is low (Figure 6A). The sixty Sgr@Swir values vary from 0.05 to 0.75. They are presented as a function of porosity (Figure 8A). This Sgr@Swir-porosity plot presents the same three SgrM-porosity trends put in evidence in our previous paper[1; 2].

 - In the high porosity region, Sgr@Swir is scattered from 0.25 to 0.45;
 - In the low porosity region, Sgr@Swir *vs* porosity plot presents two different trends.
   Values either increase (FTB) or decrease (argillaceous sandstone) as porosity decreases.

Most of the Sgr@Swir values are equal or close to SgrM whatever the Swir values (Figure 8B). This result implies that Sgr@Swir-porosity plot is the same as SgrM-porosity plot. In a different manner, this implies Sgr@Swir values, as SgrM ones, are controlled only by rock characteristics, and not by Swir values.

In the following, we verify whether the main relationships established with SgrM in previous paper[1; 2] still hold with Sgr@Swir values and we compare experimental values with values calculated with simplifed Land's law.

Relationship with Other Parameters

Some key relationships are presented hereafter: Sgr@Swir versus permeability (Figure 8C), clay content (Figure 8D), T2 mean (Figure 9A) and CBW (Figure 9B). The CBW cut-off is equal to 3.3 ms as in the previous paper [2]. As shown before [2], CBW is a function of microporosity content and T2 mean of pore size. Then, microporosity and pore size control Sgr@Swir values (Figure 9A and B). Figure 9C shows Sgr@Swir as a function of Swir. The scatter is quite significant and it is also confirmed by literature data (Figure 9D).

It is concluded that the main relationships established with SgrM in our previous paper [1; 2] still hold with Sgr@Swir values.

Comparison with Land's Law Results

In 1968, Land [11] proposed a hyperbolic law to estimate Sgr values from Sgi values, based on Swir and Sgr@Swir values. His aim was the calculation of end points of relative permeability curves. He has first proposed this law with six experimental relationships of the literature [11]. Later, Land has validated this relationship with his own experimental data [17] measured on two samples: one Berea sandstone the porosity of which is 0.25, and one alundum plug with a 0.45 porosity. Originally, the Land's law is limited from 0 to 1-Swir (equation 1). Usually, a simplified form is used (equation 3). This form is not limited to 1-Swir and allows to calculate Sgr@Swir value with SgrM and Swir ones. Because of the hyperbolic form of Land's law, estimated Sgr values are different according to the simplified and original Land's laws (Figure 10A). This also implies that SgrM value is different from Sgr@Swir value. The difference between the two parameters is a function of Swir values (Figure 10B); unlike we have shown previously with experimental data.

The sixty experimental Sgr@Swir values have been compared to calculated va lues with equation 4 based on Land's law interpretation. The difference between calculated Sgr@Swir values and those measured exhibits a mean error around to 0.04 and a maximum error close to 0.08 (Figure 11A). This systematic error remains even if uncerta inty of Swir is included (points Swir_min and Swir_max). In very low and high Sgr@Swir region, the error is small because of respectively low Sgr@Swir values and very low Swir values. In the first region, as corresponding SgrM values are also low, the Land 's law using may lead to large relative errors.

So, except the lowest Swir values, the error induced by the simplified Land's law is not negligible. The best estimation of Sgr@Swir parameter is to accept the SgrM value (Figure 11B).

DISCUSSION

Most of the previous authors have not clearly distinguished initial gas saturation and irreducible water saturation. Within a reservoir, the initial gas saturation may vary either with the height above the free water level for a given rock quality, or with the rock quality at a given distance above the initial contact. In the former case, the dependency of Sgr on Sgi has been recognised [11] and is revisited in a companion paper [19]. This paper presents only results about irreducible gas saturation that is the latter case.

The relationship between Sgr@Swir and Swir is quite scattered. This confirms the conclusions presented by Chierici et al. [8] who failed to reveal a relationship between Sgr(Swir) and Swir, based on 250 samples. One of the main reasons is that Swir is a conventional parameter the value of which is linked to experimental conditions: highest used capillary pressure. Other studies illustrated that such a relationship might exist on small data sets [12, 18]. It might indicate that such a trend does not hold on larger data sets incorporating a large range of rock qualities.

It should be pointed out that the very close agreement between Sgr@Swir and SgrM values obtained from our large data set (Figure 8B), confirms some previous experimental conclusions [3, 7, 14] achieved on smaller sets of samples. This implies Sgr@Swir is strongly dependent on porosity and the amount of microporosity in the same way as SgrM. These experimental observations suggest that the specific parameter, Sgr@Swir, is not a function of irreducible water saturation, but depends mainly on rock quality.

CONCLUSIONS

- The fluid distribution after controlled evaporation was checked with NMR and X-ray scanner measurements and found homogeneous;

- The Sgr values obtained by evaporation-imbibition were found in very close agreement with those achieved by capillary drainage-imbibition on eight reservoir samples;

- The presence of irreducible water prior to the imbibition does not change the existence of two opposite Sgr trends as a function of porosity (or permeability);

- Sgr at irreducible water saturation may decrease as porosity decreases. This relationship is shown to be related to increasing clay content, decreasing pore size or increasing amount of microporosity in particularly the part that is linked to the clay content;

- Sgr may either increase or decrease as a function of irreducible water saturation, showing that Sgr is not controlled only by initial water saturation;

- Maximum trapped gas saturation and Sgr at irreducible water saturation were found equal. So, the frequent extrapolation of Land's empirical relationship to the interval [SgrM, Sgr@Swir] is not correct.

NOMENCLATURE

Kg: intrinsic permeability estimated with gas

Phi: porosity

C: Land's constant

CBW: clay bound water (fraction of Vp)

Sgi: initial gas saturation

Sgr: residual gas saturation

S^*_{gi}: effective initial gas saturation

S^*_{gr}: effective residual gas saturation

Sgr@Swir: residual gas saturation of sample at Swir

SgrM: maximum residual gas saturation

Swir: irreducible water saturation

T2: NMR transverse relaxation time (ms)

T2mean: logarithmic mean of NMR transverse relaxation time (ms)

ACKNOWLEDGEMENTS

REFERENCES

1. Suzanne K., Hamon G., Billiotte J., Trocme V., "Distribution of trapped gas saturation in heterogeneous sandstone reservoirs", *SCA* (2001), **SCA2001**-14, 12p.

2. Hamon G., Suzanne K., Billiotte J., Trocme V., "Field-wide variations of trapped gas saturation in heterogeneous sandstone reservoirs"; *SPE* (2001), **SPE 71524**, 13p

3. Geffen T.M., Parish D.R., Haynes G.W., Morse R.A., "Efficiency of gas displacement from porous media by liquid flooding", *Trans. AIME*, (1952), **v 195**, pp 29-38

4. Crowell D.C., Dean G.W., Loomis A.G., "Efficiency of gas displacement from a water-drive reservoir", *Report of investigations*, (1966), **6735 USBM,** pp 1- 29

5. Delclaud J., "Laboratory measurements of the residual gas saturation", Second European *Core Analysis Symposium*, pp 431-451

6. Katz D.L., Legatski M.W., Tek M.W., Gorring M.R., Neilsen R.L., "How water displaces gas from porous media", *Oil and Gas Journal* (Jan., 1966), pp 55-60

7. Mc Kay B.A., "Laboratory studies of gas displacement from sandstone reservoirs having strong water drive", *APEA Journal*, (1974), pp 189-194

8. Chierici G.L., Ciucci G.M., Long G., "Experimental research on gas saturation behind the water front in gas reservoirs subjected to water drive", *World Petroleum Congress*, (June 1963) **sec II-17**, PD6, pp 483-498

9. Keelan D.K., "A practical approach to determination of imbibition gas-water relative permeability", *SPE-AIME*, (Feb. 1976), **SPE 4988**, pp 199-204

10. Jerauld G.R., "Gas -oil relative permeability of Prudhoe bay", *SPE* (1996), **SPE 35718**, pp 653-670

11. Land C.S., "Calculation of imbibition relative permeability for two and three phase flow from rock properties"; *SPEJ* (June 1968), **v8**, n 2, pp 149-156

12. Agarwal R.G., Alhussainy R., Ramey H.J. Jr., "Importance of water influx in gas reservoirs"; *Journal of Petroleum Technology* (1965), **SPE 1244**, pp 1336-1342,

13. Adams S.J., Farmer R.G., Hawon D., Seybold O., "Laboratory and in situ determination of residual gas saturations in Maui"; (2000) *New Zealand petroleum conference proceedings* (19-22 march 2000), 6 p.

14. Firoozabadi A., Olsen G., Van Golf-Racht T., "Residual gas saturation in water-drive gas reservoirs"; SPE - AIME (1987), **SPE 16355**, pp 319-327

15. Hamon G., "Two-Phase Flow Rock-Typing: Another Perspective."; **SPE 84035***, 2003*

16. Monicard M., *Cours de production, tome 1 : caractéristiques des roches réservoirs, Analyse des carottes*; Publications de l'Institut Français du Pétrole, cours de l'ENSPM, ed. Technip Paris, (1981); 203 p.

17. Land C.S., "Comparison of calculated with experimental imbibition relative permeability", *SPE (*1971) **SPE 3360**, pp 419-425

18. Skauge A., Ottesen B., "A summary of Experimentally Derived Relative Permeability and Residual Saturation on North Sea Reservoir Cores"; *SCA* (2002) **SCA2002** – 12, 12p

19. Suzanne K., Hamon G., Billiotte J., Trocm e V., "Experimental relationships between residual gas saturation and initial gas saturation in heterogeneous sandstone reservoirs."; **SPE 84038**, *2003*

20. Suzanne K., *Evaluation de la saturation résiduelle en gaz de grès mouillables à l'eau – influences des caractéristiques de la roche et de la saturation initiale en gaz* ; PhD - Ecole des Mines de Paris (2003); 150p.

TABLES

Table 1: Petrophysical description of the sample used for tomographic study.

Sandstone	Phi	Kg	RhoS	SgrM	Swir	T2 moy
Fontainebleau	0.11	385 mD	2.65 g/cm^3	0.62	0.15	280 ms

Table 2: Tomographic images obtained from a Fontainebleau Sandstone sample at various Sgi values resulting from controlled evaporation.

IMAGE				
Saturation	Sgi = 1 (Dry)	Sgi =1- Swi = 0.85	Sgi = 0.35	Sgi = 0
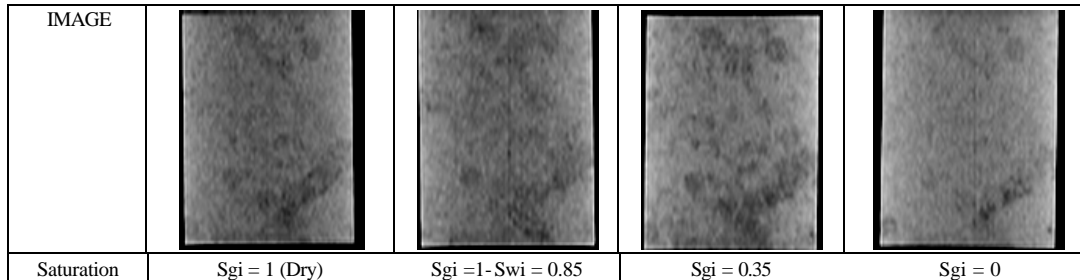
FIGURES

Figure 1: Literature data about Sgr@Swir against Swir (A) and against SgrM (B) measured on sandstones.
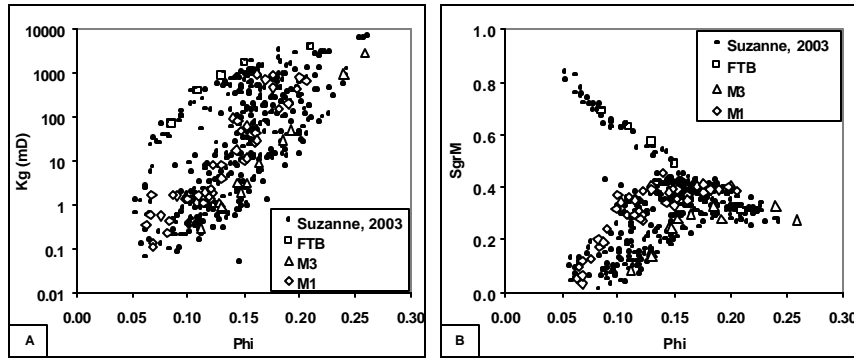
Figure 2: Samples characteristics (A) porosity against permeability; (B) porosity against SgrM.
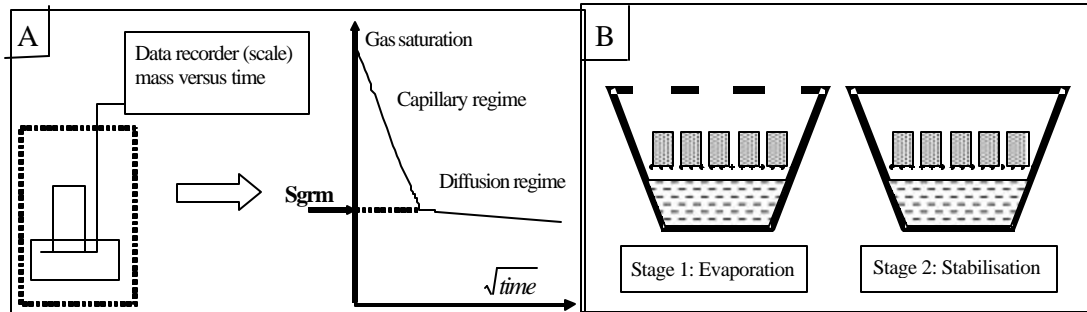
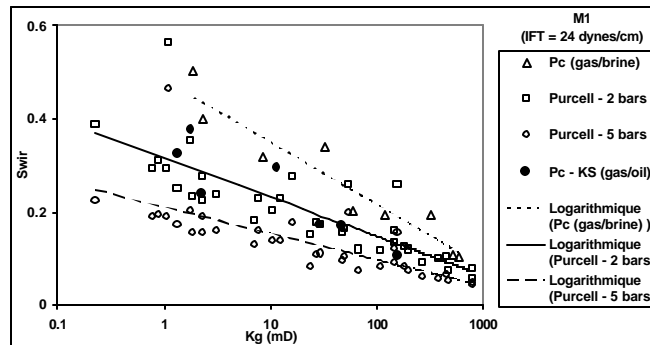Figure 3: Principle of (A) measurement of Sgr, (B) getting to Sgi (2 stages).

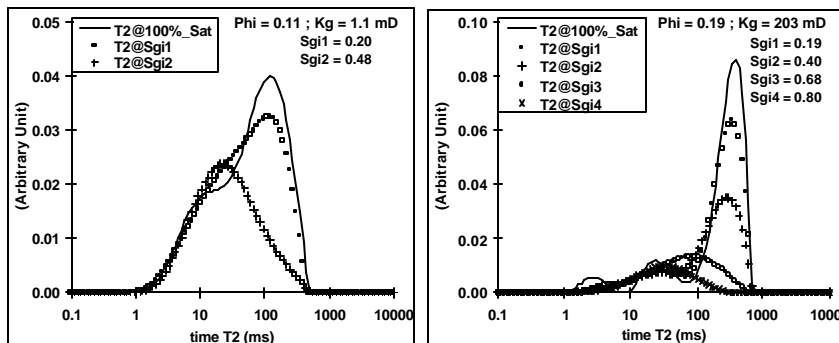Figure 4: Swir against gas permeability; our measurements are notifying "Pc – KS".

Figure 5: Fluid distributions estimated by NMR at different Sgi after controlled evaporation.
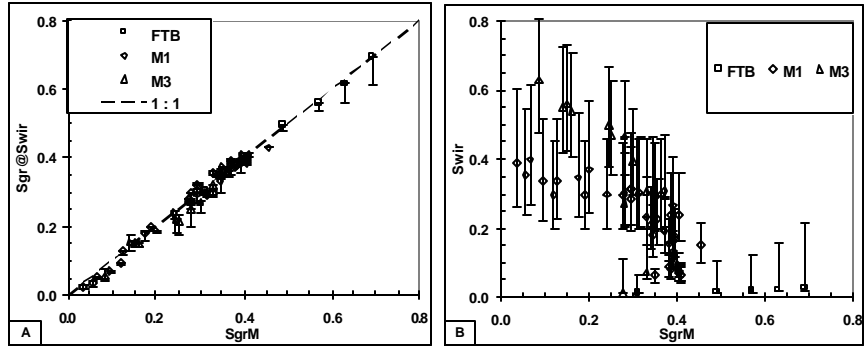

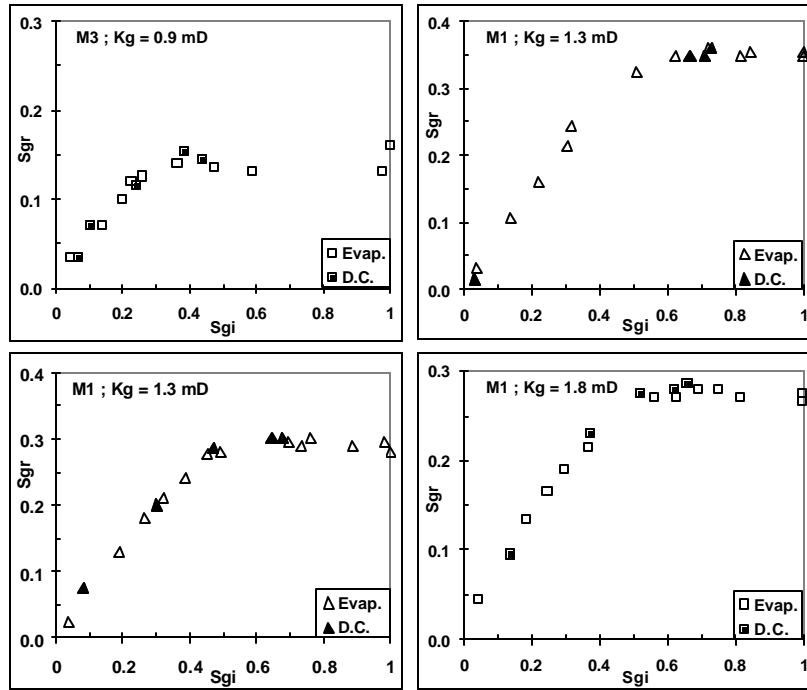Figure 6: (A) Sgr@Swir values and uncertainty intervals (B) Swir values and uncertainty intervals.

Figure 7: Four examples of relationships obtained by controlled evaporation -spontaneous imbibition (Evap.) and by capillary desorption-spontaneous imbibition (D.C.) on height core samples.
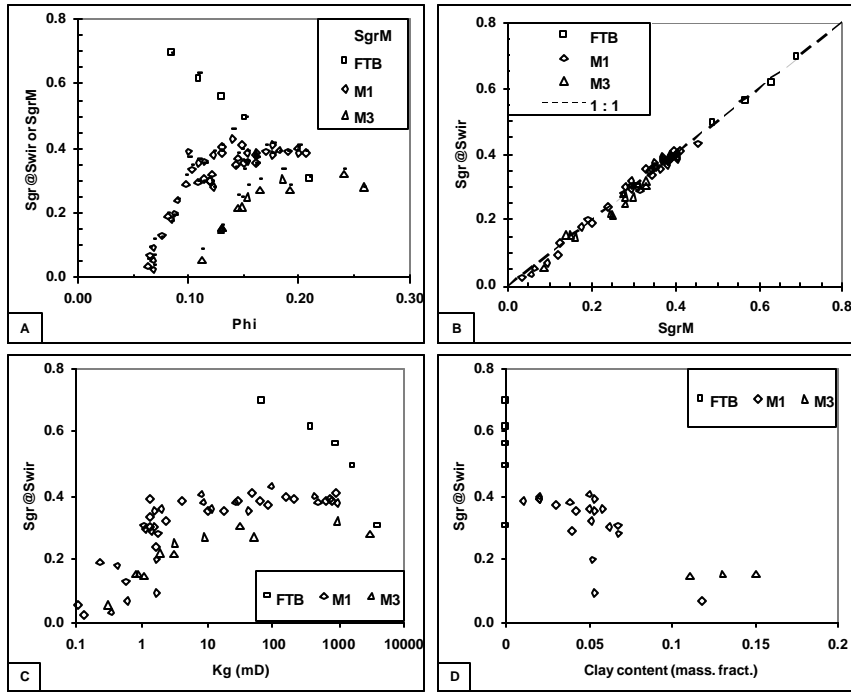
Figure 8: Relationships between Sgr@Swir and porosity (A), SgrM (B), permeability (C) and clay content (D).
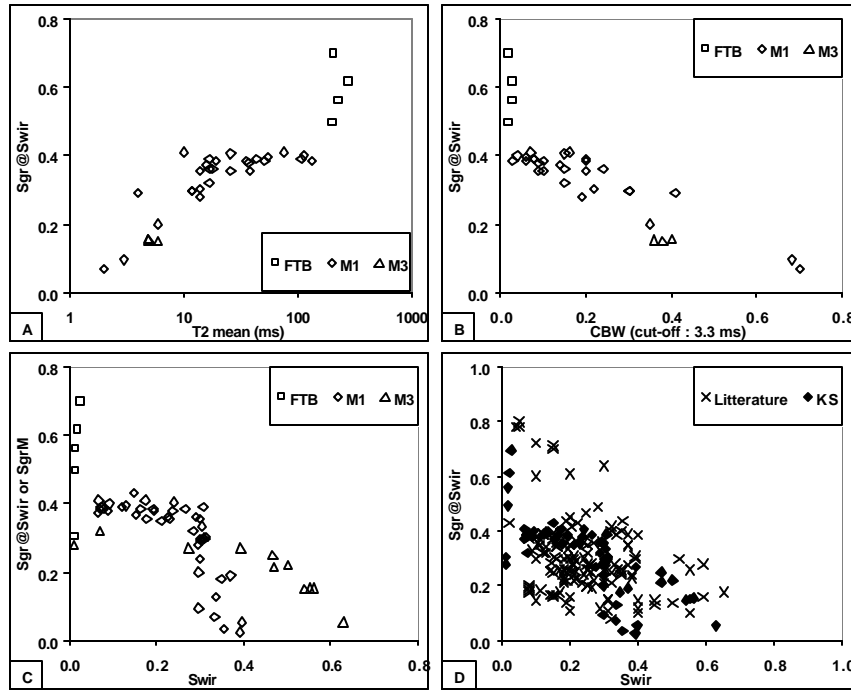

Figure 9: Relationships between Sgr@Swir and T2mean (A), Clay Bound Water (CBW) (B), Swir (C & D).
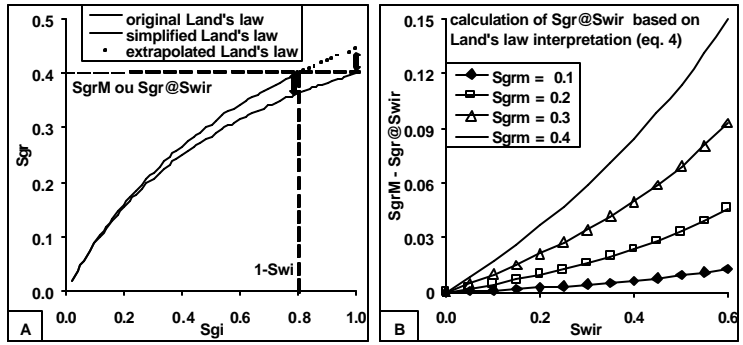
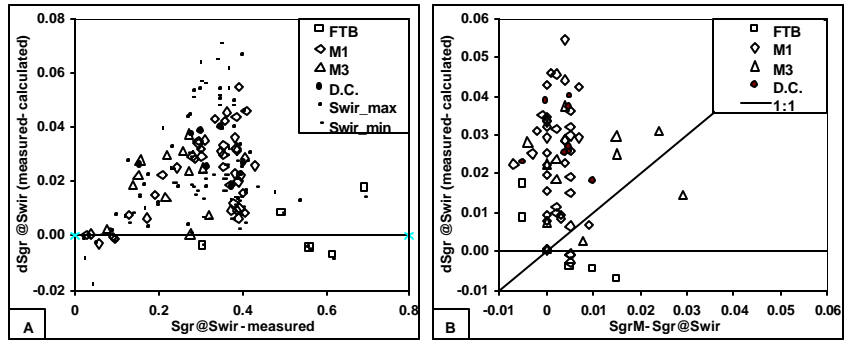Figure 10: Form of various interpretations of Land's law (A), and Sgr@Swir as a function of Swir values (B).

Figure 11: Comparison between measured Sgr@Swir and calculated Sgr@Swir based on Land's law (eq. 4). Difference between calculated and measured values (A) compared to errors if Sgr@Swir = SgrM (B).